PNAS PLUS

# Epidermal Wnt/β-catenin signaling regulates adipocyte differentiation via secretion of adipogenic factors

Giacomo Donati[a,b], Valentina Proserpio[c,1], Beate Maria Lichtenberger[a,1], Ken Natsuga[b,d], Rodney Sinclair[e], Hironobu Fujiwara[b,f,2,3], and Fiona M. Watt[a,2,3]

[a]Centre for Stem Cells and Regenerative Medicine, Kings College London, London SE1 9RT, United Kingdom; [b]Cancer Research UK Cambridge Research Institute, Cambridge CB2 0RE, United Kingdom; [c]European Bioinformatics Institute, Wellcome Trust Sanger Institute, Wellcome Trust Genome Campus, Hinxton CB10 1SD, United Kingdom; [d]Department of Dermatology, Hokkaido University Graduate School of Medicine, Sapporo 060-8638, Japan; [e]University of Melbourne and Epworth Hospital, Melbourne, VIC, Australia; and [f]Laboratory for Tissue Microenvironment, RIKEN Center for Developmental Biology, Kobe, Hyogo 650-0047, Japan

Edited by Elaine Fuchs, The Rockefeller University, New York, NY, and approved February 28, 2014 (received for review July 9, 2013)

**It has long been recognized that the hair follicle growth cycle and oscillation in the thickness of the underlying adipocyte layer are synchronized. Although factors secreted by adipocytes are known to regulate the hair growth cycle, it is unclear whether the epidermis can regulate adipogenesis. We show that inhibition of epidermal Wnt/β-catenin signaling reduced adipocyte differentiation in developing and adult mouse dermis. Conversely, ectopic activation of epidermal Wnt signaling promoted adipocyte differentiation and hair growth. When the Wnt pathway was activated in the embryonic epidermis, there was a dramatic and premature increase in adipocytes in the absence of hair follicle formation, demonstrating that Wnt activation, rather than mature hair follicles, is required for adipocyte generation. Epidermal and dermal gene expression profiling identified keratinocyte-derived adipogenic factors that are induced by β-catenin activation. Wnt/β-catenin signaling-dependent secreted factors from keratinocytes promoted adipocyte differentiation in vitro, and we identified ligands for the bone morphogenetic protein and insulin pathways as proadipogenic factors. Our results indicate epidermal Wnt/β-catenin as a critical initiator of a signaling cascade that induces adipogenesis and highlight the role of epidermal Wnt signaling in synchronizing adipocyte differentiation with the hair growth cycle.**

skin | niche cross-talk | stem cells

Mammalian skin is a complex organ composed of a variety of cell and tissue types, including interfollicular epidermis, hair follicles (HFs), melanocytes, nerves, blood vessels, muscles, fibroblasts, and adipocytes. The development and patterning of these cells and tissues are governed by intercellular communication (1–3).

One well-known example of this communication is the link between the HF growth cycle and the oscillation in thickness of the dermal adipocyte layer (4–6). When HFs grow deep into the dermal adipocyte layer in the anagen (growth) phase of the cycle, the adipocyte layer dramatically increases in thickness. This event reflects both increased adipogenesis and hypertrophy of individual adipocytes (7). When HFs regress (catagen phase) and enter the resting (telogen) phase, the adipocyte layer becomes thinner. The growth cycle of rodent HFs is coordinated to form waves of hair growth that traverse the body and the thickness of the skin adipocyte layer oscillates in synchrony with these waves (3).

The synchronized patterns of HF growth and expansion of dermal fat correlate with the activation of the canonical Wnt pathway, which is well established to positively regulate anagen (3, 8). Expression of bone morphogenetic protein 2 (Bmp2) in the mature dermal adipocyte layer is inversely correlated with Wnt activity and inhibits HF growth (3). There is also evidence that immature dermal adipocytes activate HF stem cells to initiate the hair growth cycle (7). These reports suggest that the adipocyte differentiation process is a natural on-off cycling switch for the regulation of hair growth. Although the mechanisms of HF regulation by adipose tissues have been described, it is unknown whether the HF regulates the morphogenesis, differentiation, and thickness of the dermal adipocyte layer.

In this study, we examined the role of epidermal Wnt/β-catenin signaling in regulating the dermal adipocyte layer and demonstrate that Wnt-dependent epidermal secreted factors promote adipocyte formation.

## Results

**Thickness of the Adipocyte Layer Correlates with Hair Growth in Mouse and Human Skin.** We quantified the volume of the dermal adipocyte layer (hypodermis) in dorsal mouse skin during the first 80 d of postnatal life (Fig. 1*A*). We confirmed that the adipocyte layer increased in thickness during HF morphogenesis, corresponding to the first anagen [postnatal day (P)10–P15], and decreased dramatically towards the following telogen (P23) (Fig. 1*A*). During the second anagen (P33), the volume of the adipocyte layer again increased and then decreased with the onset of the second telogen (P68). The increase in adipocyte thickness during the first postnatal HF regeneration happened during the transition from telogen to early anagen, and there was no change during later anagen (Fig. S1 *A* and *B*). The thickness of the adipocyte layer correlated with the hair cycle even when hair growth became asynchronous in older mice (Fig. S1 *C–E*). In addition, the volume of the adipocyte layer in telogen skin increased as mice aged (Fig. S1 *E* and *F*).

To examine whether there was also a relationship between HFs and adipocyte layer thickness in human skin, we compared

### Significance

**The synchronized patterns of hair follicle growth and expansion of the dermal adipocyte layer have long been recognized. Although factors secreted by adipocytes are known to regulate the hair growth cycle, it is unclear whether, conversely, the epidermis can regulate adipogenesis. Our study now demonstrates that activation of epidermal Wnt/β-catenin signaling stimulates adipocyte differentiation in vivo and in vitro. The effect can be mediated by secreted factors, including insulin-like growth factor 2 and bone morphogenetic proteins 2 and 6.**

Author contributions: G.D. and H.F. designed research; G.D., V.P., B.M.L., and H.F. performed research; G.D., K.N., R.S., H.F., and F.M.W. contributed new reagents/analytic tools; G.D., H.F., and F.M.W. analyzed data; and G.D., H.F., and F.M.W. wrote the paper.

The authors declare no conflict of interest.

This article is a PNAS Direct Submission.

Freely available online through the PNAS open access option.

[1]V.P. and B.M.L. contributed equally to the work.

[2]H.F. and F.M.W. contributed equally to the work.

[3]To whom correspondence may be addressed. E-mail: hfujiwara@cdb.riken.jp or fiona.watt@kcl.ac.uk.

This article contains supporting information online at www.pnas.org/lookup/suppl/doi:10.1073/pnas.1312880111/-/DCSupplemental.

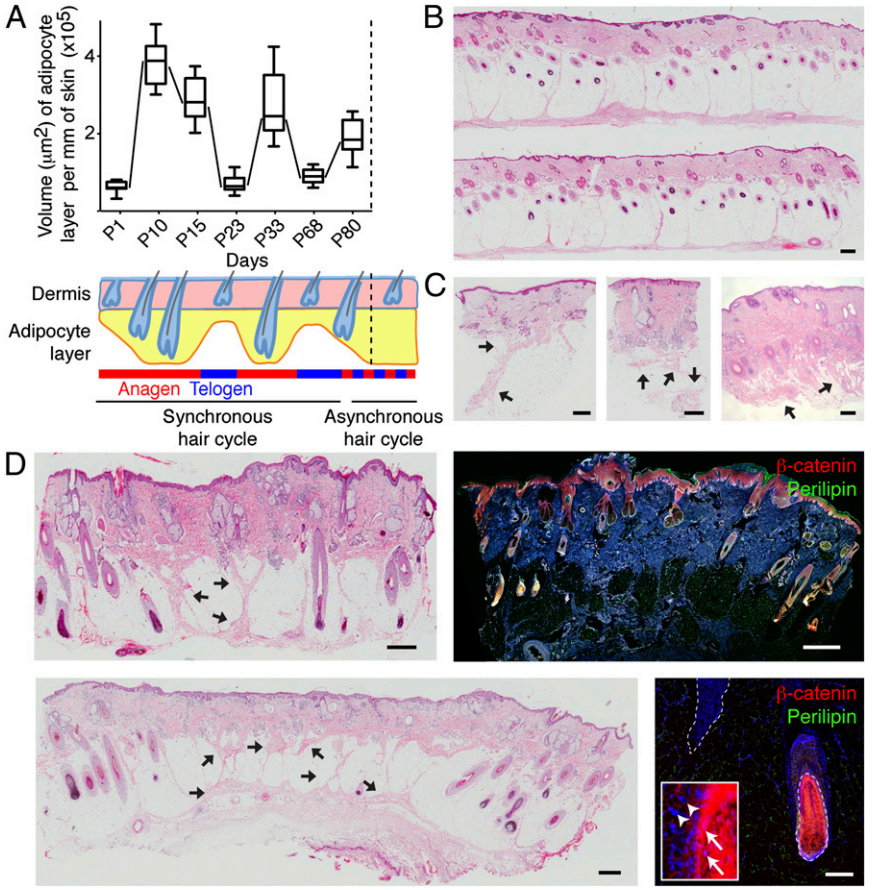


**Fig. 1.** Relationship between hair follicle growth and the thickness of the dermal adipocyte layer. (*A*) Quantification of adipocyte layer thickness in P1-P80 mice. Diagram shows corresponding status of the hair growth cycle. Data are median and 25th and 75th percentile from three mice per time point. (*B–D*) H&E-stained human adult scalp skin from healthy (*B*), alopecia areata (*C*), and sebaceous nevus (*D*) patients. (Scale bar, 500 μm.) (*D*) (*Right*) Sections of human sebaceous nevus were immunostained for β-catenin (red) and Perilipin (green) with DAPI counterstain (blue). White arrows in the *Inset* indicate nuclear β-catenin, which is absent in the cells indicated by arrowheads. (Scale bars, 500 μm; except 100 μm in *Lower Right*.)

normal hairy scalp (Fig. 1*B*) with scalp from three patients with alopecia areata (Fig. 1*C*) and two with sebaceous nevus (Fig. 1*D*). In contrast to mice, human dermis is organized into regular lobules of mature adipocytes surrounded by fibroblasts as shown by H&E and Perilipin [a marker of differentiated adipocytes (9)] staining. In pathological samples, these reticular fibroblast networks became more pronounced while the total thickness of the adipocyte layer decreased (Fig. 1 *C* and *D*, arrows). We quantitated dermal thickness in adjacent affected and unaffected skin in one alopecia areata patient who had not received any treatment for the condition (Fig. 1*C, Right*) and one case of sebaceous nevus (Fig. 1*D, Lower*). In each case, the thickness of the fat layer was decreased by 50% in the regions of hair loss (from ∼2 to 1 mm). In healthy human anagen HFs, as in the mouse, nuclear β-catenin was present in hair bulb keratinocytes, which were surrounded by Perilipin-positive mature adipocytes (Fig. 1*D, Right*). Given the small number of samples analyzed and the complexity of the diseases etiology, we cannot establish a direct link between hair loss and adipocyte thickness in human skin. Nevertheless, regions of hair loss were correlated with reduced adipocyte layer thickness in the samples we examined.

**Inhibition of Epidermal Wnt Signaling Results in a Reduction in the Adipocyte Layer in Adult and Embryonic Skin.** Activation of Wnt signaling stimulates HFs to enter anagen and can reprogram cells in adult interfollicular epidermis to form ectopic follicles and differentiate along the HF lineages (10, 11). To investigate whether Wnt/β-catenin signaling in the epidermis affects the hypodermis, we examined the skin of K14ΔNLef1 transgenic mice that express N-terminally deleted Lef1 (ΔNLef1), which lacks the β-catenin binding site, under the control of the Keratin 14 promoter (12). The keratin 14 promoter is active in the epidermal basal keratinocyte compartment but not in the dermis. ΔNLef1 acts as a dominant-negative inhibitor of Wnt/β-catenin signaling. HF morphogenesis occurs normally in K14ΔNLef1 mice, and expression of Wnt target genes is unaffected at P1 (Fig. S2 *A* and *B, Left*). However, the follicles subsequently convert into epidermal cysts with ectopic sebocytes and Wnt signaling is inhibited at the base of the residual hair follicles (Fig. S2*B*, *Right*) (12).

Taking into account that the onset of the first postnatal anagen is delayed in mutant mice (12), we compared the thickness of the dermal adipose layer of WT and K14ΔNLef1 mice during the same hair cycle phase. K14ΔNLef1 dermal adipose volume was increased in conjunction with the growth of HFs as in WT mice. However, at all time points except P1, the Perilipin-positive adipocyte layer was thinner than in WT mice (Fig. 2*A* and Fig. S2*A*). This phenotype became more prominent as mice aged (Fig. 2 *A* and *B*).

The reduction in thickness of the adipocyte layer corresponded to an increase in the lower, reticular, dermal layer that is rich in fibrillar collagen (Fig. 2 *B* and *C*). K14ΔNLef1 epidermal cysts in the deep dermis were surrounded by reticular dermis rather than mature adipocytes (Fig. 2*C*, arrows).

The histological observations were confirmed by immunostaining adult mouse skin with antibodies to markers of adipocytes

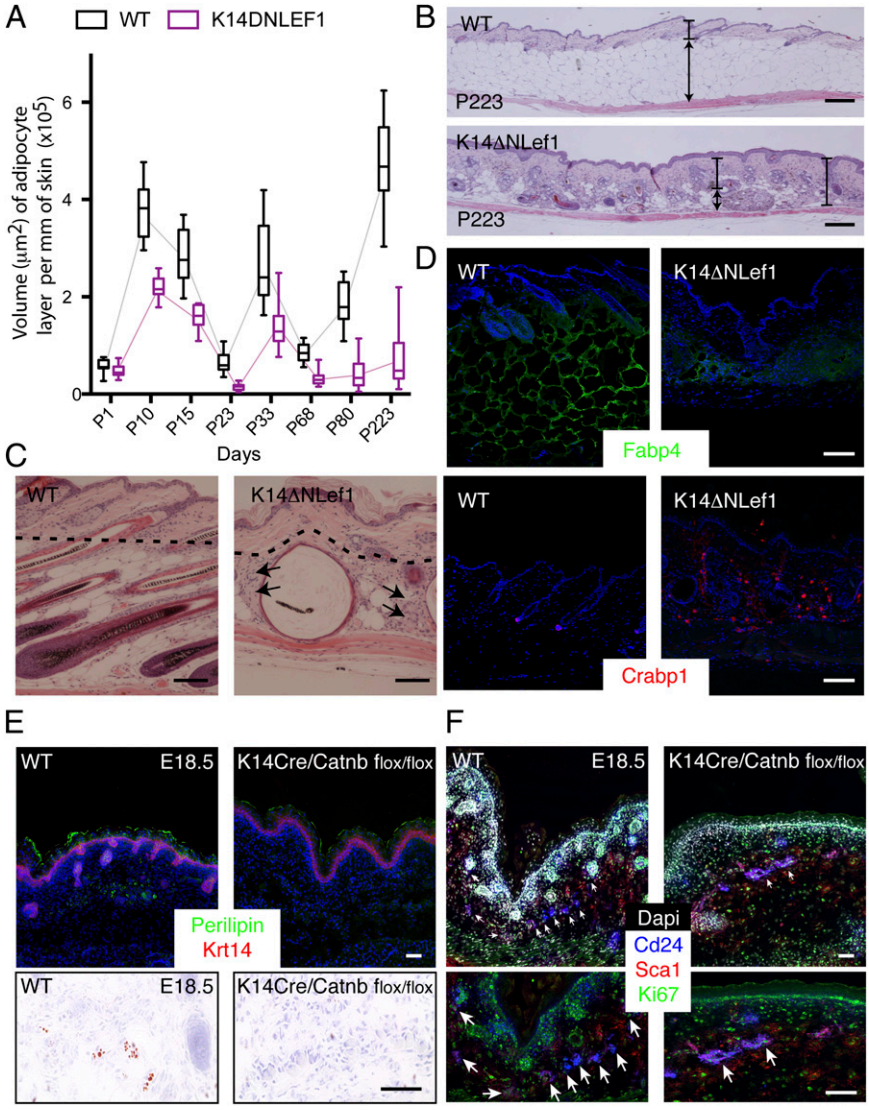


**Fig. 2.** Inhibition of epidermal Wnt/β-catenin signaling impairs adipogenesis during hair follicle morphogenesis and regeneration. (*A*) Quantification of adipocyte layer thickness in WT and K14ΔNLef-1 skin. Data are median and 25th and 75th percentile from three mice per time point. (*B* and *C*) H&E-stained dorsal skin of WT and K14ΔNLef-1 mice at P223 (telogen) (*B*) and P150 (*C*). Double-headed arrows (*B*) indicate adipose thickness, whereas bars indicate dermis. In *C*, arrows show fibroblasts surrounding cysts and dotted lines indicate border between permanent and transient portions of HFs. (*D*) Sections of adult WT and K14ΔNLef-1 skin immunostained for Fabp4 (green) and Crabp1 (red), with DAPI counterstain (blue). (*E*) Sections of embryonic WT and K14Cre/Catnb flox/flox skin immunostained for Perilipin (green) and Krt14 (red), with DAPI counterstain (blue) (*Upper*) or stained with Oil red O (*Lower*). (*F*) Embryonic WT and K14Cre/Catnb flox/flox skin immunostained for Ki67 (green), Sca1 (red), and Cd24 (blue), with DAPI counterstain (white). White arrows indicate cluster of Cd24/Sca1$^+$ cells. [Scale bars, 300 (*B*), 100 (*C* and *D*), and 25 μm (*E* and *F*).]

and fibroblasts. There was a striking decrease in Perilipin and Fabp4 [another marker of differentiated adipocytes (13)] positive cells in K14ΔNLef1 compared with WT skin (Fig. 2*D* and Fig. S2*A*, *Right*). This decrease correlated with an increase in cellular retinoic acid binding protein 1 (Crabp1) expression. In WT adult skin, Crabp1 expression is restricted to the dermal papilla cells. In contrast, as previously reported (14), Crabp1 was widely expressed in the dermis of K14ΔNLef1 skin (Fig. 2*D*). However, flow cytometric analysis of adipocyte precursor cells (Sca1$^+$Cd24$^+$) (7) revealed no significant difference between WT and transgenic adult skin (Fig. S2 *C* and *D*).

To inhibit epidermal Wnt signaling during skin morphogenesis, we ablated β-catenin in embryonic skin via K14Cre. This resulted in a loss of Perilipin-positive, lipid-positive adipocytes (Fig. 2*E*). In WT skin, small clusters of Sca1/Cd24 double-positive cells were associated with the growing HFs at embryonic day (E)18.5. On removal of epidermal β-catenin, Sca1/Cd24 double-positive cell clusters were still present in the lower dermis (Fig. 2*F*).

We conclude that epidermal β-catenin signaling is critical for adipocyte differentiation during development and that epidermal inhibition of Wnt/β-catenin activity in adult epidermis decreases the thickness of the adipose layer, due to a decrease in mature adipocytes. Although the increase in thickness of the adipose layer during normal mouse skin aging can have a number of underlying causes (15), our observations on K14ΔNLef1 skin suggest an ongoing contribution of Wnt signaling (Fig. 2*A*).

**Activation of Wnt/β-Catenin Signaling in Adult Epidermis Induces Adipocyte Formation.** To examine whether activation of epidermal β-catenin signaling stimulates adipogenesis, we used K14ΔNβ-cateninER transgenic mice, in which stabilized, active β-catenin is fused with the C terminus of a mutant estrogen receptor under the

control of the Keratin 14 promoter (11). Wnt/β-catenin signaling in keratinocytes is activated by topical application of 4-hydroxytamoxifen (4OHT) to mouse dorsal skin. A single application to telogen skin is sufficient to stimulate anagen, whereas six treatments not only stimulate anagen of existing follicles but also induce ectopic HF formation as a result of expansion of the epidermal stem cell compartment and reprogramming cells in the sebaceous gland and interfollicular epidermis to differentiate along the hair follicle lineages (9).

Early anagen WT and K14ΔNβCateninER skin was treated with two doses of 4OHT skin (at P23 and P25) and analyzed at full anagen (P32 and P38). Although there was a transient increase in $Cd24^{+}Sca1^{+}$ adipocyte progenitors (P32 only) on transgene activation, the thickness of the adipocyte layer was unaffected (Fig. S3 *A* and *B*). The lack of the effect of the transgene is consistent with the known role of endogenous Wnt activation in promoting anagen (16). To examine whether signals originating from the epidermis can reset the adipocyte oscillation cycle, we next induced precocious activation of epidermal Wnt/β-catenin signaling. Application of one dose of 4OHT to telogen (7–11 wk old) transgenic mice led to induction of anagen and a marked expansion of the adipocyte layer (Fig. 3 *A* and *B*). There was no effect on the number of adipocyte precursors (Fig. 3*B*), but there was an increase in differentiated, Perilipin-positive adipocytes (Fig. 3*B*). When ectopic HF formation was induced by repeated applications of 4OHT, adipocytes were found in the upper dermis, where they are normally absent (Fig. 3*A*, arrows).

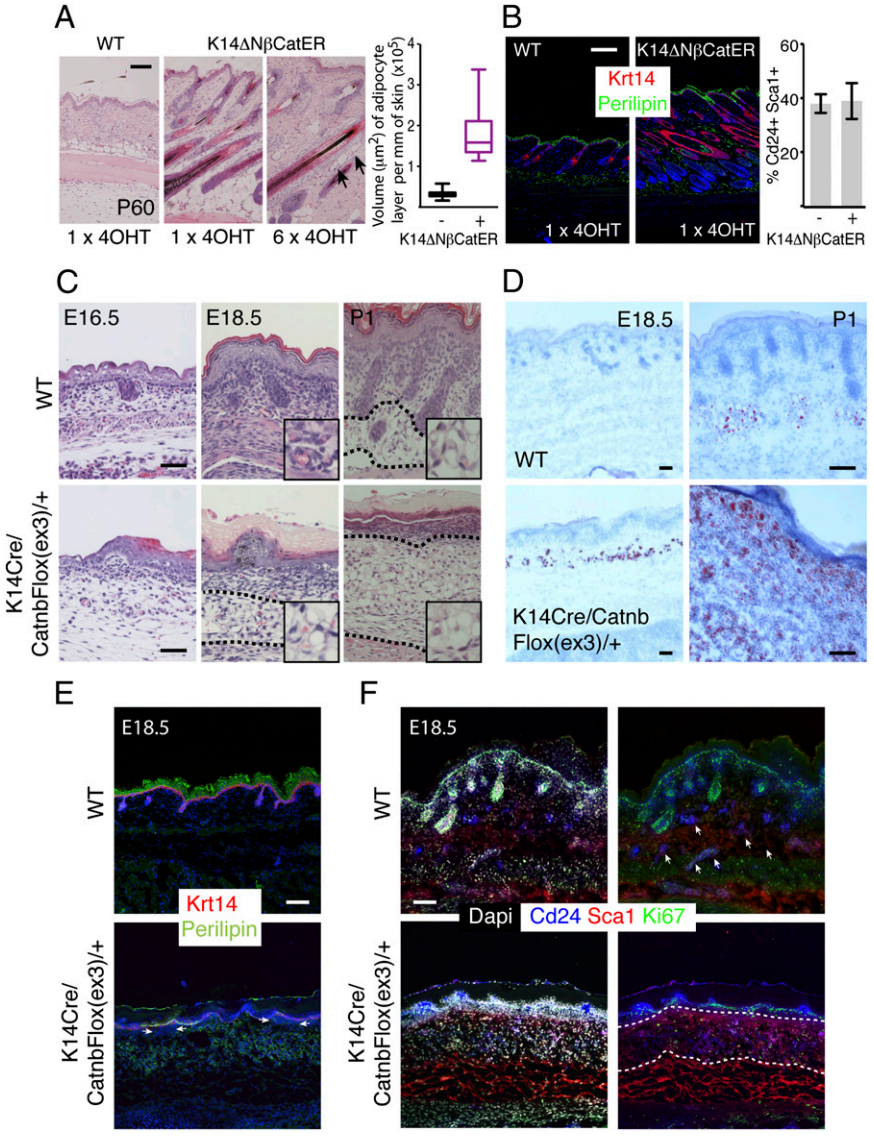


**Fig. 3.** Activation of epidermal Wnt/β-catenin signaling promotes dermal adipocyte formation. (*A*) H&E-stained sections of WT or K14ΔNβ-cateninER (K14ΔNβCatER) dorsal skin treated with one or six doses of 4OHT in telogen (P60). Arrows indicate ectopic adipocyte formation in upper dermis. Graph shows quantification of adipocyte layer thickness after 1 dose of 4OHT. Data are median and 25th and 75th percentile from three mice. (*B*) Sections of WT or K14ΔNβ-cateninER skin immunostained for Perilipin (*green*) and Krt14 (*red*) with DAPI counterstain (*blue*). (*B*) (*Right*) Flow cytometry of Sca1/Cd24 double-positive dermal cells after 1 dose of 4OHT. Data are mean ±SD from three mice. (*C*) H&E-stained dorsal skin of WT and K14Cre/CatnbFlox(ex3)/+ mice. *Insets* show magnified images of lower dermis. (*D–F*) WT and K14Cre/CatnbFlox(ex3)/+ dorsal skin sections stained for Oil Red O (*D*), Perilipin (green), and K14 (red), with DAPI counterstain (blue) (*E*) or Ki67 (green), Sca1 (red), and Cd24 (blue), with DAPI counterstain (white) (*F*). White arrows indicate dermal condensate (*E*) or cluster of $Cd24/Sca1^{+}$ cells (*F*). Areas surrounded by black dotted lines are filled by differentiated adipocytes, whereas white dotted lines surround adipocyte precursors. [Scale bars, 100 (*A* and *B*) and 50 μm (*C–F*).]

We conclude that activation of Wnt/β-catenin signaling in adult epidermis stimulates adipogenesis in association with induction of anagen and ectopic HF formation.

**Activation of Wnt/β-Catenin Signaling in Embryonic Epidermis Induces Adipocyte Differentiation.** To examine whether epidermal Wnt/β-catenin signaling directly stimulated dermal adipocyte formation, rather than indirectly via stimulation of hair growth, we generated K14Cre/CatnbFlox(ex3)/+ mice in which HF morphogenesis fails (17). These mice express stabilized, N-terminally truncated β-catenin in K14-positive epidermal basal keratinocytes. The K14 promoter becomes active in embryonic epidermis by E11.5 (17). During normal dorsal skin development in WT mice, mature adipocytes are readily detected from P1, and some cells with characteristic lipid vacuoles can be seen as early as P1 (E20.5) (areas between dotted lines and *Insets* in Fig. 3*C*), correlating with HF morphogenesis and activation of epidermal Wnt/β-catenin signaling (18). In K14Cre/CatnbFlox(ex3)/+ mice, cells with lipid vacuoles were already visible by E18.5, and large numbers of adipocytes were present at P1 (areas between dotted lines and *Insets* in Fig. 3*C*). The embryos died perinatally, allowing us to assess only developmental phenotypes.

To confirm the histological findings, we labeled sections for lipid, Perilipin, Fabp4, and Pparγ (19). K14Cre/CatnbFlox(ex3)/+ mice exhibited adipocyte differentiation in E18.5 skin and a massive increase in the number of adipocytes at P1 (Fig. 3*D*). Adipocytes were found throughout the dermis (Fig. 3*D*). In WT skin, expression of Perilipin, Fabp4, and nuclear Pparγ was mainly detectable at P1, whereas in transgenic mice, these markers were widely expressed at E18.5 and P1 (Fig. 3*E* and Fig. S3*C*). Sca1, a marker of pre- and mature adipocytes (13), was expressed in a similar pattern to Fabp4 (Fig. S3*C*). Conversely, in WT P1 skin, many fibroblasts, especially in proximity to the epidermal basement membrane, expressed Crabp1, whereas expression was reduced in K14Cre/CatnbFlox(ex3)/+ mice (Fig. S3*C*). In K14Cre/CatnbFlox(ex3)/+ skin, there was also a massive increase of $Cd24^{+}Sca1^{+}$ preadipocytes (area between dotted lines) associated with stimulation of proliferation in the dermis (Fig. 3*F*).

These results indicate that activation of epidermal Wnt/β-catenin signaling during development induces adipogenesis in the absence of HF morphogenesis.

**Epidermal Wnt/β-Catenin Signaling Promotes Adipocyte Differentiation via Secretion of Ligands for BMP and Insulin Pathways.** Given that the epidermis and dermis are separated by a basement membrane, the inductive effect of epidermal Wnt/β-catenin signaling on adipocyte differentiation is most likely achieved by secreted factors. We searched for candidate factors by analyzing previously published gene expression profiles (9) generated from triplicate age-matched adult K14ΔNβ-cateninER mice that were either treated with vehicle alone (telogen) or received one dose of 4OHT (to induce anagen) or six doses (to induce anagen and ectopic follicles). We did not compare gene expression data from transgenic mice treated with a single dose of 4OHT and anagen WT mice and therefore could not evaluate the extent to which the two situations are similar. Epidermal cells and dermal cells were flow sorted from the skin of each mouse and also compared with cells from triplicate neonatal WT mice (P2) (9). Overrepresentation analysis of gene ontology (GO) terms revealed that the category "extracellular region" was strongly enriched in the sets of genes that were differentially expressed (DEG) in the epidermis on 4OHT-induced activation of the Wnt pathway (Fig. 4*A*). The presence of a large number of secreted proteins (Table 1) highlights the potential complexity of communication between keratinocytes and neighboring cells.

In the fibroblast dataset, the "lipid metabolic process" and "cell differentiation" GO categories were highly represented in the DEG, together with the previously reported "cell proliferation" GO term (9) (Fig. 4*B*). We looked specifically at genes involved in the transcriptional regulation of adipocyte differentiation (20, 21). The master regulators Pparγ and Cebpα were significantly up-regulated. One of their upstream regulators,

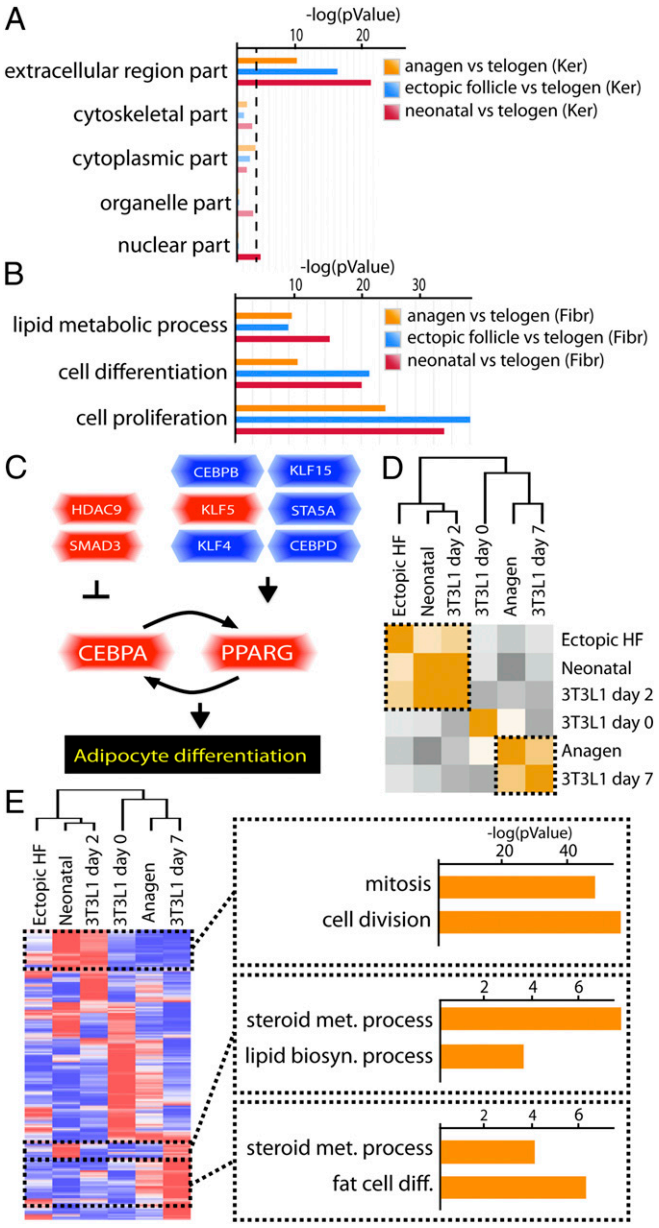


**Fig. 4.** GO analysis of gene expression profiles of epidermal and dermal cells from K14ΔNβ-cateninER mice. (*A*) GO overrepresentation analysis of DEG in keratinocytes from K14ΔNβ-cateninER mice (only GO terms related to protein localization). Samples from adult anagen skin (one dose of 4OHT), adult anagen skin with ectopic HFs (six doses of 4OHT), and neonatal skin were compared with adult telogen skin (9). (*B*) GO overrepresentation analysis of DEG in fibroblasts from K14ΔNβ-cateninER mice. (*C*) Gene expression pattern of transcriptional regulators of adipocyte differentiation. Up- (red) and down- (blue) regulated genes in fibroblasts when epidermal Wnt/β-catenin signaling was activated are shown. (*D*) Heat map display of hierarchical clustering (Pearson correlation, positive in orange, negative in grey) of fibroblast DEG (neonatal, anagen, and ectopic follicles) and 3T3-L1 adipocyte differentiation markers (25). (*E*) Z-score heat map representing DEG as in *D*. Low expressed genes are in blue, high expressed in red. GO analysis of specific clusters is shown.

**Table 1. Secreted proteins differentially expressed between growing and resting hair follicles**

| Gene Categories | Up-regulated in growing hair follicles | Down-regulated in growing hair follicles |
|---|---|---|
| Extracellular matrix | Col4a1(A,E,N), Col12a1(A), Col18a1(A,N), Col4a2(A,N), Lamc1(N), Col4a3(E), Col27a1(E,N), Col5a1(E,N), Col14a1(E,N), Col11a1(N), Fbn2(E,N), Col5a2(N), Col2a1(E), Lamb1-1(A,N), Lama2(N), Col6a2(N), Emid1(E,N), Col8a1(E,N), Pcolce(N), Bgn(A,E,N), Fbln1(N), Fmod(N), Tnc(A,E,N), Vcan(N), Npnt(E), Olfml2a(N), Olfml2b(N), Spon1(A,E), Nid1(N), Nid2(N), Bcan(N), Hspg2(N) | Col8a2(A,N), Col27a1(A), Pcolce2(A,E,N), Egfl6(N), Fbln7(A,E,N), Spock2 (A,E,N), Tgfbi(E), Pcolce(E), Ecm1(N) |
| Peptidases and peptidaes inhibitors | Adamts16(A,N), Adamts20(A,E,N), Adamts5(A,N), Adamtsl1(N), Cpxm1(A,E,N), Itih5(N), Klk7(A,E,N), Klk8(N), Pappa(A,E), Pcsk5(A,N), Pi15(A,E), Prss35(N), Serpine2(E,N), Tmprss11e(E) | Adam23(E), Adamtsl4(E,N), Angptl4(E,N), C2(A,E), Cpxm2(E), C3(E,N), C4b(E,N), Ctla2a(N), Htra1(A,E), Klk11(A,E), Loc100046035(E), Mmp12(A,E,N), Pm20d1(N), Prss23(A,E,N), Serpinb2(A,E,N), Timp2(N) |
| Defense response cytokines and chemokines | Ccl12(N), Cxcl14(N), Il1f5(N), Eda(E), Penk(E,N), Lipg(E,N), Pla2g7(A,E,N), Il1rap (N) | Ccl27a(E,N), Ccl8(A,E,N), Ccl9(A,E,N), Cxcl10(N), Cxcl12(N), Cxcl9(A,E,N), Grem1(A,N), Il1b(A,E,N), IL33(A,E,N), Il34(A,E), Xcl1(N), Il7(A,E,N), Pf4(A,E), Lipm(A,E,M), Il1rn(E), Il4ra(E,N), Il15ra(A,E,N), Il22ra2(A,E), Tnfrsf11b(N), Lepr(A,E,N), Tnfrsf18(N), C1qb(A,E), Cd163(A,E,N), C9(A,E,N), Fcgr2b(A,N), Defb1(A,E), B2m(N), Defb6(A,E,N), Smpdl3a(N), Smpdl3b(N) |
| Growth factors | Artn(N), Bmp6(A,E), Fgf5(A,E,N), Gdf10(A,E), Igf2(N), Igfbp2(N), Igfbp5(N), Ltbp1(E), Mdk(N), Ngf(N), Pdgfa(N), Wnt10b(N), Tgfb3(E), Wnt16(N), Tgfb2(E,N), Wnt4(N), Wnt5b(A,E), Wnt6(E,N), Wnt7a(N), Sfrp2(N), Sema3a(E,N), Hhip(E), Sema3b(E,N), Sema3f(N), Edn1(N), Edn2(A,E) | Fgf18(E,N), Ctgf(A,E,N), Fgfbp1(A,E), Figf(A,E,N), Igfbp3(E,N), Igfbp4(N), Kazald1(A,E,N), Ltbp2(A,E,N), Nrg4(A,E,N), Bmp1(N), Ptn(N), Wnt3(A,E), Dkk3(N), Sema3c(A,E), Sema3d(A,E) |
| Others | Agrp(A,N), Chi3l1(A), Coch(E), Egfl8(N), Lgi1(N), Egflam(N), Fam20a(A), Fam20c(N), Fstl1(E,N), Gpc3(N), Vash1(N), Vwa2(E), Krtdap(N), Lepre1(N), Lgals1(N), Lgi2(N), Lox(N), Lypd6(N), Mup1-2–3(A), Kcp(A,E,N), Nppc(A), Nptx2(N), Nts(N), Pcsk5(A,N), Pthlh(E,N), Ptx3(N), S100a9(N), Scrg1(A) | Angptl7(A,E,N), Amy1(N), Bche(N), Cck(A,E,N), Chit1(A,E,N), Chl1(A,N), Cilp(N), Creg1(A,E,N), Cxadr(N), Efemp1(E), Fam132a(N), Lum(A,E), Fam3c(A,E), Gm885(E), Gm94(N), Gpha2(A,E,N), Gsn(N), Xdh(N), Hsd17b13(A,E,N), Sectm1b(E,N), Loc100046120(E,N), Sepp1(N), Sectm1a(A,E,N), Vit(E,N), Acpp(N), Lgals3bp(A,E,N), Myoc(A,E,N), Retnla(A,E,N), Sbsn(N), Npc2(A,E), |

A, anagen; E, ectopic HF; N, neonatal.

Klf5, was also increased, whereas the others were decreased (Fig. 4*C*). These observations indicate that epidermal Wnt signaling stimulates adipocyte differentiation and also indicate some heterogeneity in the dermal cell response.

3T3-L1 cells are a well-characterized in vitro model of adipogenesis (22, 23). Differentiation is characterized by an early phase of clonal expansion followed by terminal differentiation (24). To further understand fibroblast responses to epidermal Wnt activation, we compared fibroblast DEG from neonatal, adult anagen, and ectopic follicle-bearing skin with DEG of differentiating 3T3-L1 cells (25). This analysis revealed that fibroblasts from ectopic follicle and neonatal skin were more similar to the early phase of 3T3-L1 differentiation (day 2), whereas adult anagen fibroblasts resembled fully differentiated adipocytes (day 7) (Fig. 4*D*). To characterize these correlations further, we performed GO analysis on the common gene clusters: adult anagen and 3T3-L1 day 7 cells shared a gene set enriched for "steroids metabolic processes" and "fat cell differentiation," whereas neonatal fibroblasts and 3T3-L1 day 2 cells shared a gene set enriched for "mitosis" and "cell division" (Fig. 4*E*). In addition, neonatal fibroblasts and 3T3-L1 day 7 cells were enriched for genes involved in "steroids metabolic process" and "lipid biosynthesis process" (Fig. 4*E*). These results suggest that neonatal fibroblasts correspond to an earlier stage of adipogenesis, whereas in adult anagen, maturation of adipocytes is taking place.

We routinely culture keratinocytes on an irradiated feeder layer of J2 Swiss mouse 3T3 cells (26). The feeder layer of K14Cre/CatnbFlox(ex3)/+ keratinocytes contained many cells with large lipid vacuoles, whereas that of WT keratinocytes did not (Fig. 5*A*). To establish experimentally whether β-catenin activation stimulates keratinocytes to secrete adipogenic factors, we cultured 3T3-L1 cells in methylisobutylxanthine, dexamethasone, and insulin adipocyte differentiation medium (22) and medium conditioned by keratinocytes from WT, K14Cre/CatnbFlox(ex3)/+, or K14ΔNLef1 mice. Six days later, we examined lipid production by Oil Red O staining and quantitative RT-PCR (qRT-PCR) of genes that are known to be up- (Leptin, Adiponectin, Pparγ, and Fabp4) or down- (Pref-1) regulated during adipocyte differentiation (Fig. 5 *B–D*).

3T3-L1 cells exposed to K14Cre/catnbFlox(ex3)/+ keratinocyte conditioned medium exhibited greater and more rapid adipogenesis than those exposed to WT keratinocyte medium (Fig. 5*C*). Conversely, medium conditioned by K14ΔNLef1 keratinocytes inhibited adipogenesis (Fig. 5*D*). When sparse preadipocyte 3T3-L1 cells were treated with conditioned medium, there was no effect on growth rate (Fig. S4). These data suggest that Wnt/β-catenin regulates epidermal production of factors that stimulate adipocyte differentiation.

To identify secreted factors that affect adipocyte differentiation, we tested a panel of 14 candidate factors that were identified from the K14ΔNβ-cateninER expression profile or significantly down-regulated in keratinocytes expressing ΔNLef1 or up-regulated in K14Cre/CatnbFlox(ex3)/+ embryonic epidermis. Three factors stimulated 3T3-L1 differentiation: Bmp2, Bmp6, and insulin-like growth factor-2 (Igf2) (Fig. 6 *A* and *B*). Consistent with these observations, differentiation of 3T3-L1 cells in the presence of WT keratinocyte conditioned medium was stimulated, in a dose-dependent manner, by exogenous insulin, whereas the effect of insulin was much less pronounced in conditioned medium of K14Cre/CatnbFlox(ex3)/+ keratinocytes (Fig. 6*C*). In addition, pharmacological inhibition of BMP signaling (27) significantly decreased the adipogenic effect of K14Cre/CatnbFlox(ex3)/+ keratinocyte conditioned medium (Fig. 6*D*).

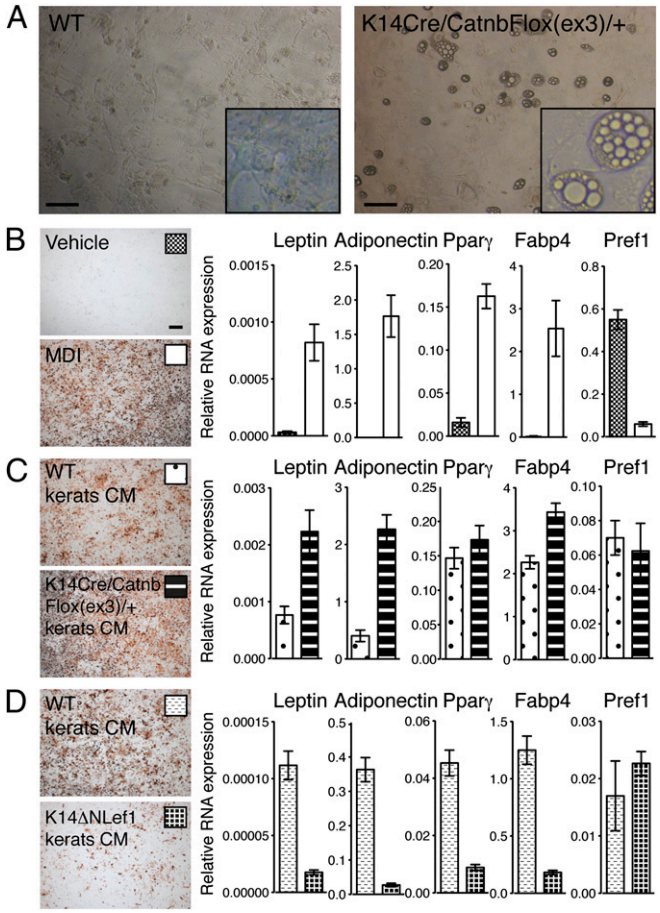


**Fig. 5.** Wnt/β-catenin signaling in keratinocytes regulates adipocyte differentiation through secreted factors. (*A*) Phase contrast images of 3T3-J2 cocultured with WT or K14Cre/CatnbFlox(ex3)/+ keratinocytes for 6 d. *Insets* are higher magnification views of 3T3-J2 cells. (*B–D*) Differentiation of 3T3-L1 cells in MDI medium (*B*), MDI medium conditioned by keratinocytes from WT or K14Cre/CatnbFlox(ex3)/+ mice (*C*), or K14ΔNLef-1 mice (*D*) for 6 d. Cells were stained with Oil Red O (*Left*). Gene expression levels of adipocyte markers (Leptin, Adiponectin, Pparγ, and Fabp4) and a preadipocyte marker (Pref1) in 3T3-L1 cells were examined by qRT-PCR. Data are mean ± SD from three independent wells. [Scale bars, 100 (*A*) and 200 μm (*B–D*).]

These in vitro results demonstrate that activation of epidermal Wnt/β-catenin signaling can induce adipocyte differentiation by stimulating secretion of ligands for the BMP and insulin signaling pathways.

## Discussion

It has long been recognized that the HF growth cycle and oscillation in the thickness of the skin adipocyte layer are synchronized. Recently, adipocyte-derived factors have been reported to regulate the hair growth cycle (3, 7). Our study now identifies activation of Wnt/β-catenin signaling in keratinocytes as a trigger for adipocyte differentiation, suggesting that periodic activation of epidermal Wnt/β-catenin signaling during the hair cycle contributes to the synchrony.

HF formation was not required for induction and expansion of dermal adipocytes during skin morphogenesis (Fig. 2). In addition, Wnt/β-catenin activation in cultured keratinocytes stimulated differentiation of 3T3-L1 cells into mature adipocytes in vitro (Fig. 5). These findings indicate that Wnt/β-catenin activation in keratinocytes, rather than HF formation per se, promotes adipocyte differentiation. Our observations provide an explanation for why adipocytes still form in hairless skin, such as the paw skin. It remains possible that adipocyte development in embryonic skin and changes in adipocyte thickness in adult skin rely on different signaling pathways and that only the embryonic stage relies directly on epidermal Wnt signaling. In vitro coculture of 3T3 cells and keratinocytes may mimic the developmental stage rather than the adult situation.

During mouse skin morphogenesis, activation of Wnt/β-catenin signaling and formation of HFs are observed by E14.5, whereas commitment to the adipocyte lineage occurs at E16.5 (28). This timing suggests that epidermal Wnt/β-catenin signaling is the initial signal that promotes dermal adipogenesis, rather than adipocytes initiating HF formation. When β-catenin was deleted in embryonic epidermis, CD24/Sca1$^+$ adipocyte precursors were still detectable, suggesting that the lack of adipocytes is due to a block in terminal differentiation. When epidermal β-catenin was activated in embryonic and adult skin, there was an expansion of differentiated adipocytes. These results are consistent with recent evidence that epidermal β-catenin activation leads to expansion of both the upper and lower dermal lineages (28).

In adult skin, ectopic activation of epidermal Wnt/β-catenin signaling (Fig. 3) or transplantation of adipocyte precursors into the dermis (7) leads to expansion of the adipocyte layer or HF anagen, respectively. These findings suggest that both the epidermis and the adipose layer can initiate the positive feedback loop linking hair cycle progression to adipocyte differentiation. It will be interesting to determine the entity of the clock that regulates the timing and duration of hair growth cycle and other associated cyclic regenerative events in the skin.

Activation of Wnt/β-catenin signaling in keratinocytes led to the expression of a diverse set of secreted factors. Among them, we validated Igf2 and Bmp6 as factors that promote adipogenesis in vitro and also confirmed a role for Bmp2 (17, 20, 21). Although we have not determined the sites of expression of these factors during skin morphogenesis and hair follicle cycling, there are indications that they are expressed in the hair follicle (3, 29, 30). In addition, expression of several components of the Igf signaling pathway are altered in skin aging, when the adipocyte layer increases in thickness (15). It is notable that Bmp2, Igf2, and the hair cycle regulator Pdgfa are expressed both by adipocytes and epidermal cells (3, 7, 9), pointing to the complexity of communication between the epidermis and adipocyte layer.

Bmp signaling is known to be important for the functional identity of the dermal papilla (31). The activation of epidermal Wnt/β-catenin signaling during development also induces widespread dermal condensate formation (17) (Fig. 3*E*, white arrows) and in adulthood leads to expansion of the papillary and reticular dermis (28). Therefore epidermal Wnt affects multiple dermal compartments, indicative of both short and long range signaling.

A balance between pro- and anti-adipogenic signals must be required for spatiotemporal regulation of adipogenesis, and indeed, our gene expression profiles included some antiadipogenic factors (21). Conditioned medium from K14ΔNLef1 keratinocytes inhibited 3T3-L1 adipocyte differentiation, suggesting that they secrete inhibitors of adipogenesis. Because activation of Wnt signaling in keratinocytes influences the behavior of melanocytes, nerves, and fibroblasts (9, 17, 32), some of the antiadipogenic factors may primarily regulate other cell populations in the skin.

In conclusion, our data highlight the role of epidermal Wnt signaling in adipocyte morphogenesis and synchronizing adipocyte differentiation with HF growth. Further studies are necessary to identify the upstream master clock regulators controlling the timing and duration of hair growth cycle and, in particular, whether long-range regulation (neuronal, systemic or hormonal) is involved. There are several physiological and anatomical advantages of synchronizing the HF growth cycle with oscillations in thickness of the adipocyte layer. The combination of a high density of hairs and dermal adipocytes insulates the body from the cold. In addition, the down growth of the HF during

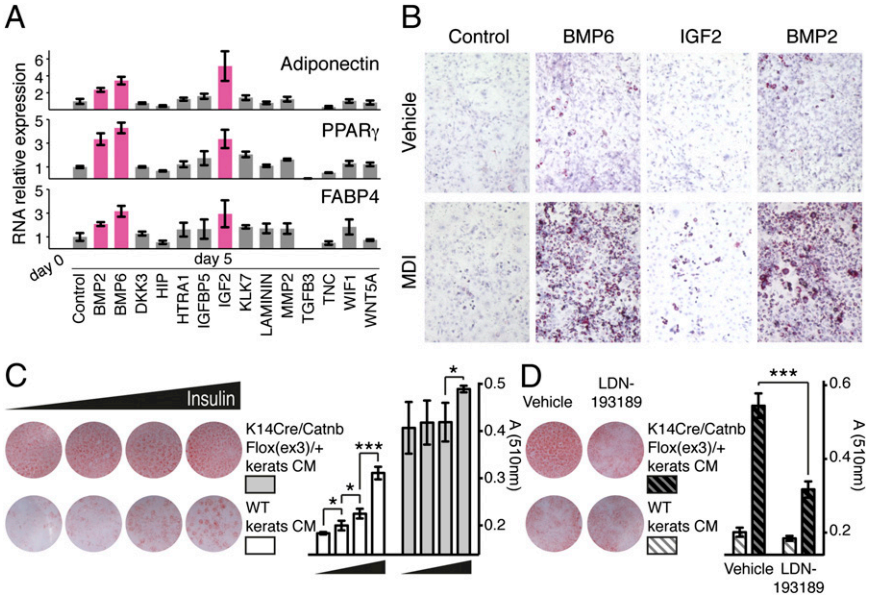


**Fig. 6.** Identification of epidermal adipogenic factors. (*A*) qRT-PCR of Adiponectin, Pparγ, and Fabp4 expression in 3T3-L1 cells after 5 d of exposure to adipogenic medium containing the indicated recombinant proteins. Data are mean ± SD from three independent wells. (*B*) 3T3-L1 cells stained with Oil Red O after 7 d of exposure to the proteins indicated in the absence (*Upper*) or presence (*Lower*) of adipogenic medium. (*C*) Effect of different insulin concentrations on 3T3-L1 preadipocyte differentiation induced by MDI and conditioned medium from WT or K14Cre/CatnbFlox(ex3)/+ keratinocytes. Oil Red O staining and quantification (absorbance at 510 nm) are shown. Data are mean ± SD from four independent wells. (*D*) Effect of Bmp inhibition during differentiation induced by MDI adipogenic medium and conditioned medium from WT or K14Cre/CatnbFlox(ex3)/+ keratinocytes. Oil Red O staining and quantification are shown. Data are mean ± SD from four independent wells. $*P < 0.05$; $***P < 0.0005$.

anagen may be facilitated by the presence of an adipocyte layer separating the reticular dermis from the underlying striated muscle, the panniculus carnosus.

## Materials and Methods

**Mice.** All animal procedures were subject to local ethical approval and performed under a UK Government Home Office license and RIKEN's Regulations for the Animal Experiments. K14ΔNLef1, K14ΔNβ-cateninER, and Pdgfra-gfp transgenic mice have been described previously (11, 12). K14Cre/CatnbFlox (ex3)/+ and K14Cre/Catnb flox/flox mice were generated by crossing K14Cre (Jackson Laboratory) with CatnbFlox(ex3) mice (generous gift from Makoto Taketo, Department of Pharmacology, Kyoto University, Graduate School of Medicine, Kyoto) (33) and β-catenin lox/lox mice (16), respectively. The K14ΔNβ-cateninER transgene was activated by topical application of 4-hydroxytamoxifen (34). Only female mice were used for this study.

**Human Tissue.** Human tissue samples were obtained with informed consent and processed for research in accordance with the recommendations of the relevant national legislation.

**Histology, Flow Cytometry, and Staining.** Optimal cutting temperature compound or paraffin-embedded tissues were sectioned and stained by conventional methods. Primary antibodies for immunofluorescence were as follows: Perilipin A and Axin2 (Abcam); Keratin14 (Covance); Fabp4 (R&D Systems); Pparγ, Cyclin D1, and Jag1 (Santa Cruz); Sca1 and Cd24 (eBioscience); Ki67 (Novocastra) and Crabp1 (Sigma); and Krt31 (Progen). Images were acquired with a Leica TCS SP5 Tandem Scanner confocal microscope. Images of H&E-stained sections were acquired with an Aperio scan-scope, and quantification of the adipocyte layer was performed with Imagescope. The HF area within the adipocyte layer was excluded from the quantification.

For Oil Red O staining, sections or cultured cells were washed with PBS and fixed in formalin for 10 min at room temperature. Cells were incubated for 30 min at room temperature with 60% filtered Oil Red O stock solution (0.3g/100 mL of isopropanol). Sections/cells were washed with 60% (vol/vol) isopropanol and then water before visualization. Lipid levels were quantified by extracting Oil Red O stained cells with isopropanol and measuring absorbance at 510 nm.

Dermal cells for FACS analysis were isolated as described previously (9) and labeled with the following antibodies: anti–CD24-PE clone: M1/69, anti–Ly-6A/E (Sca1)-FITC or Alexa Fluor 700, anti–Cd29-FITC, anti–Cd34-APC (eBioscience), and lineage antibody mixture V450 (BD Horizon). Pdgfra cells were sorted with Anti-Cd140a-PE or APC (eBioscience) or Pdfgra-gfp. Labeled cells were analyzed on a BD LSRFortessa cell analyzer. DAPI or LIVE/DEAD Fixable Violet Dead Cell Stain (Life Technologies) was used to exclude dead cells.

**Cell Culture.** Mouse primary dorsal skin keratinocytes were cultured on 3T3-J2 feeders in calcium-free FAD medium (1 part Ham's F12, adenine $1.8 \times 10^{-4}$ M, 3 parts DMEM) supplemented with 10% FCS, hydrocortisone (0.5 μg/mL), insulin (5 μg/mL), cholera toxin (8.4 ng/mL), and epidermal growth factor (10 ng/mL) in collagen I-coated culture flasks (35, 36).

3T3-L1 preadipocytes (generous gift from Jaswinder K. Sethi, University of Cambridge Metabolic Research Laboratories, Institute of Metabolic Science, Cambridge, United Kingdom) were maintained in DMEM (10% calf serum). Forty-eight hours after confluence, differentiation was induced with DMEM supplemented with 10% FBS, 1 μM dexamethasone, 1 μg/mL insulin, and 0.5 mM 3-isobutyl-1-methylxan-thine (IBMX) (MDI medium). Two days later, the medium was replaced with DMEM (10% FBS) and was changed every 2 d. The following recombinant proteins were added every second day: Bmp2 (200 ng/mL), Bmp6 (100 ng/mL), Dkk3 (4 μg/mL), Hip (10 μg/mL), Htra1 (8 μg/mL), Igfbp5 (5 μg/mL), Igf2 (20 ng/mL), Klk7 (5 μg/mL), Laminin (10 μg/mL), Mmp2 (5 μg/mL), Tgf-β3 (50 ng/mL), Tnc (10 μg/mL), Wif1 (1 μg/mL), and Wnt5a (1 μg/mL). On day 5 after plating, the cells were harvested, and the RNA was extracted. To test the effects of insulin, 100× serial dilutions from 1 μg/mL were used to supplement the medium. The LDN-193189 Bmp inhibitor was used at final concentration of 0.1 μM. Growth rate was determined using the Incucyte real-time video imaging system.

**qRT-PCR.** Total RNA was purified with the RNeasy Mini Kit (Qiagen) with on-column DNaseI digestion according to the manufacturer's instructions. RNA (500 ng) was reverse transcribed with SuperScriptIII (Invitrogen) and random primers. cDNA (10 ng) was used for qRT-PCR with SYBR green super mix (ABI). Data represent mean values ± SD. Primers used in this study are listed in Table S1.

**GO and Clustering Analysis.** GO term enrichment analysis was performed using DAVID (http://david.abcc.ncifcrf.gov) or GeneGO pathway analysis software (https://portal.genego.com) on DEG in keratinocytes and fibroblasts that were previously identified (9). 3T3-L1 DEG at days 0, 2, and 7 from Mikkelsen et al. (25) were compared with fibroblast DEG from Collins et al. (9). Heat maps and clustering analysis were performed with GenePattern 2.0 (37).

**ACKNOWLEDGMENTS.** We acknowledge the core services of the Cancer Research UK Cambridge Research Institute, where the project was initiated, and the assistance of Charlotte Collins, Marta Lesko, Maria Mastrogiannaki, and Kai Kretzschmar, who generously provided mice/sections for research. We also thank Asako Nakagawa for technical assistance. G.D. thanks Samuel Woodhouse for daily discussions about this project. This work was supported by grants to F.M.W. from Cancer Research UK, the European Union, the Medical Research Council, and the Wellcome Trust and to H.F. from RIKEN. B.M.L. was the recipient of a Federation of European Biochemical Societies long-term fellowship. We gratefully acknowledge financial support, in the form of access to the flow facility, from the Department of Health via the National Institute for Health Research comprehensive Biomedical Research Centre award to Guy's & St Thomas' National Health Service Foundation Trust in partnership with King's College London and King's College Hospital NHS Foundation Trust.

1. Rawles ME (1963) Tissue Interactions in Scale and Feather Development as Studied in Dermal-Epidermal Recombinations. *J Embryol Exp Morphol* 11:765–789.
2. Chuong CM, et al. (2002) What is the 'true' function of skin? *Exp Dermatol* 11(2): 159–187.
3. Plikus MV, et al. (2008) Cyclic dermal BMP signalling regulates stem cell activation during hair regeneration. *Nature* 451(7176):340–344.
4. Butcher EO (1934) The hair cycles in the albino rat. *Anat Rec* 61(1):5–19.
5. Chase HB, Montagna W, Malone JD (1953) Changes in the skin in relation to the hair growth cycle. *Anat Rec* 116(1):75–81.
6. Hansen LS, Coggle JE, Wells J, Charles MW (1984) The influence of the hair cycle on the thickness of mouse skin. *Anat Rec* 210(4):569–573.
7. Festa E, et al. (2011) Adipocyte lineage cells contribute to the skin stem cell niche to drive hair cycling. *Cell* 146(5):761–771.
8. Fuchs E, Chen T (2013) A matter of life and death: Self-renewal in stem cells. *EMBO Rep* 14(1):39–48.
9. Collins CA, Kretzschmar K, Watt FM (2011) Reprogramming adult dermis to a neonatal state through epidermal activation of β-catenin. *Development* 138(23): 5189–5199.
10. Gat U, DasGupta R, Degenstein L, Fuchs E (1998) De Novo hair follicle morphogenesis and hair tumors in mice expressing a truncated beta-catenin in skin. *Cell* 95(5): 605–614.
11. Lo Celso C, Prowse DM, Watt FM (2004) Transient activation of beta-catenin signalling in adult mouse epidermis is sufficient to induce new hair follicles but continuous activation is required to maintain hair follicle tumours. *Development* 131(8): 1787–1799.
12. Niemann C, Owens DM, Hülsken J, Birchmeier W, Watt FM (2002) Expression of DeltaNLef1 in mouse epidermis results in differentiation of hair follicles into squamous epidermal cysts and formation of skin tumours. *Development* 129(1):95–109.
13. Wolnicka-Glubisz A, King W, Noonan FP (2005) SCA-1+ cells with an adipocyte phenotype in neonatal mouse skin. *J Invest Dermatol* 125(2):383–385.
14. Collins CA, Watt FM (2008) Dynamic regulation of retinoic acid-binding proteins in developing, adult and neoplastic skin reveals roles for beta-catenin and Notch signalling. *Dev Biol* 324(1):55–67.
15. Giangreco A, Qin M, Pintar JE, Watt FM (2008) Epidermal stem cells are retained in vivo throughout skin aging. *Aging Cell* 7(2):250–259.
16. Huelsken J, Vogel R, Erdmann B, Cotsarelis G, Birchmeier W (2001) beta-Catenin controls hair follicle morphogenesis and stem cell differentiation in the skin. *Cell* 105(4):533–545.
17. Zhang Y, et al. (2008) Activation of beta-catenin signaling programs embryonic epidermis to hair follicle fate. *Development* 135(12):2161–2172.
18. Alonso L, Fuchs E (2003) Stem cells of the skin epithelium. *Proc Natl Acad Sci USA* 100(Suppl 1):11830–11835.
19. Rosen ED, et al. (1999) PPAR gamma is required for the differentiation of adipose tissue in vivo and in vitro. *Mol Cell* 4(4):611–617.
20. Cristancho AG, Lazar MA (2011) Forming functional fat: A growing understanding of adipocyte differentiation. *Nat Rev Mol Cell Biol* 12(11):722–734.
21. Rosen ED, MacDougald OA (2006) Adipocyte differentiation from the inside out. *Nat Rev Mol Cell Biol* 7(12):885–896.
22. Green H, Meuth M (1974) An established pre-adipose cell line and its differentiation in culture. *Cell* 3(2):127–133.
23. Green H, Kehinde O (1975) An established preadipose cell line and its differentiation in culture. II. Factors affecting the adipose conversion. *Cell* 5(1):19–27.
24. Tang QQ, Otto TC, Lane MD (2003) Mitotic clonal expansion: A synchronous process required for adipogenesis. *Proc Natl Acad Sci USA* 100(1):44–49.
25. Mikkelsen TS, et al. (2010) Comparative epigenomic analysis of murine and human adipogenesis. *Cell* 143(1):156–169.
26. Rheinwald JG, Green H (1975) Serial cultivation of strains of human epidermal keratinocytes: The formation of keratinizing colonies from single cells. *Cell* 6(3):331–343.
27. Yu PB, et al. (2008) BMP type I receptor inhibition reduces heterotopic [corrected] ossification. *Nat Med* 14(12):1363–1369.
28. Driskell RR, et al. (2013) Distinct fibroblast lineages determine dermal architecture in skin development and repair. *Nature* 504(7479):277–281.
29. Kulessa H, Turk G, Hogan BL (2000) Inhibition of Bmp signaling affects growth and differentiation in the anagen hair follicle. *EMBO J* 19(24):6664–6674.
30. Kurek D, Garinis GA, van Doorninck JH, van der Wees J, Grosveld FG (2007) Transcriptome and phenotypic analysis reveals Gata3-dependent signalling pathways in murine hair follicles. *Development* 134(2):261–272.
31. Rendl M, Polak L, Fuchs E (2008) BMP signaling in dermal papilla cells is required for their hair follicle-inductive properties. *Genes Dev* 22(4):543–557.
32. Takeo M, et al. (2013) Wnt activation in nail epithelium couples nail growth to digit regeneration. *Nature* 499(7457):228–232.
33. Harada N, et al. (1999) Intestinal polyposis in mice with a dominant stable mutation of the beta-catenin gene. *EMBO J* 18(21):5931–5942.
34. Fujiwara H, et al. (2011) The basement membrane of hair follicle stem cells is a muscle cell niche. *Cell* 144(4):577–589.
35. Romero MR, Carroll JM, Watt FM (1999) Analysis of cultured keratinocytes from a transgenic mouse model of psoriasis: Effects of suprabasal integrin expression on keratinocyte adhesion, proliferation and terminal differentiation. *Exp Dermatol* 8(1):53–67.
36. Jensen KB, Driskell RR, Watt FM (2010) Assaying proliferation and differentiation capacity of stem cells using disaggregated adult mouse epidermis. *Nat Protoc* 5(5): 898–911.
37. Reich M, et al. (2006) GenePattern 2.0. *Nat Genet* 38(5):500–501.

# Supporting Information

## Donati et al. 10.1073/pnas.1312880111

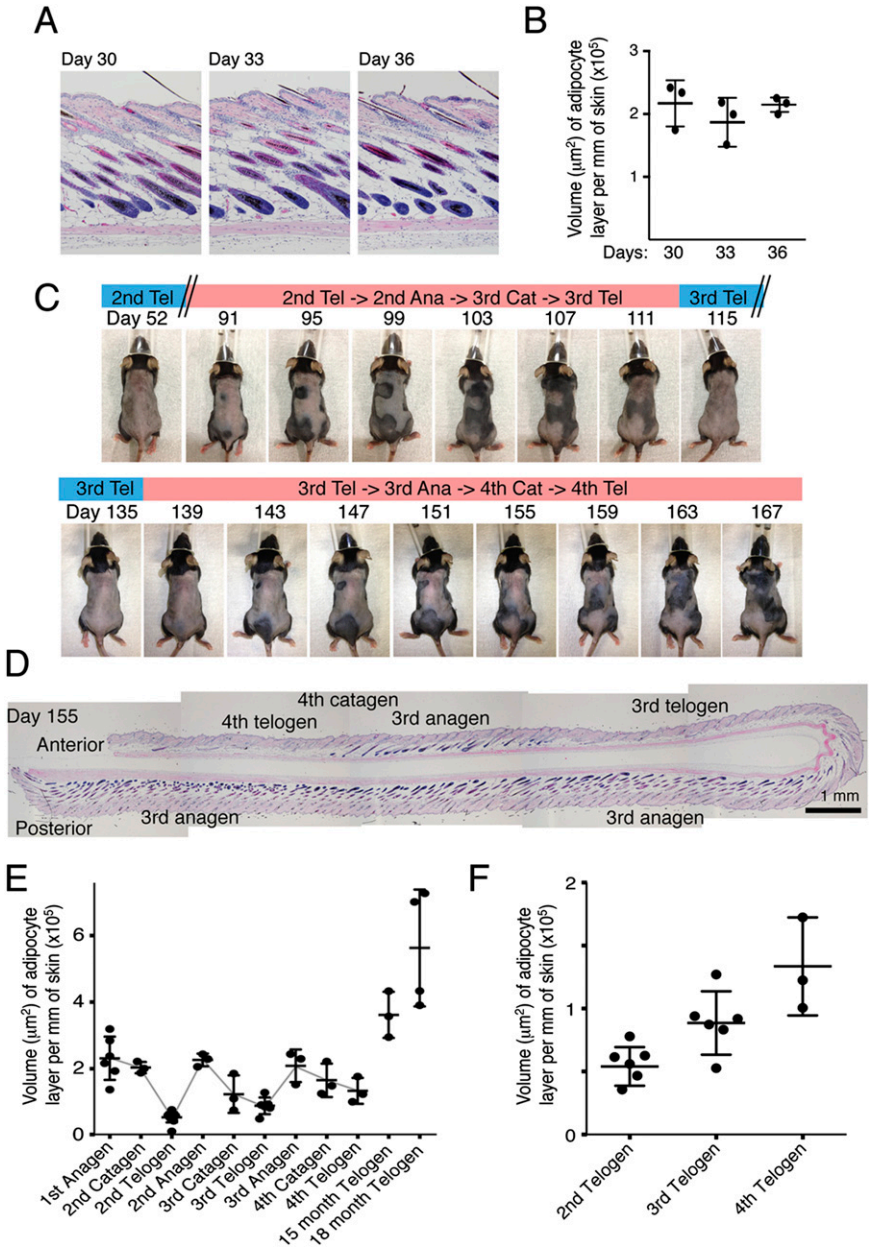


**Fig. S1.** Measurement of adipocyte layer thickness in WT mice. (*A*) Representative H&E-stained images from early, mid-, and late anagen. (*B*) Quantification of adipocyte layer thickness ($n = 3$ mice/stage). (*C*–*F*) Adipocyte layer thickness correlates with hair growth phase during asynchronous hair cycles in adult mice. (*C*) Hair cycle stages. (*D*) Representative H&E-stained image of 155-d-old mouse skin. (*E* and *F*) Quantification of adipocyte layer thickness in skin of mice aged from 2 to 18 mo ($n \geq 3$ mice/stage) (*E*) and during the second, third, and fourth telogen phases ($n \geq 3$ mice per stage) (*F*).

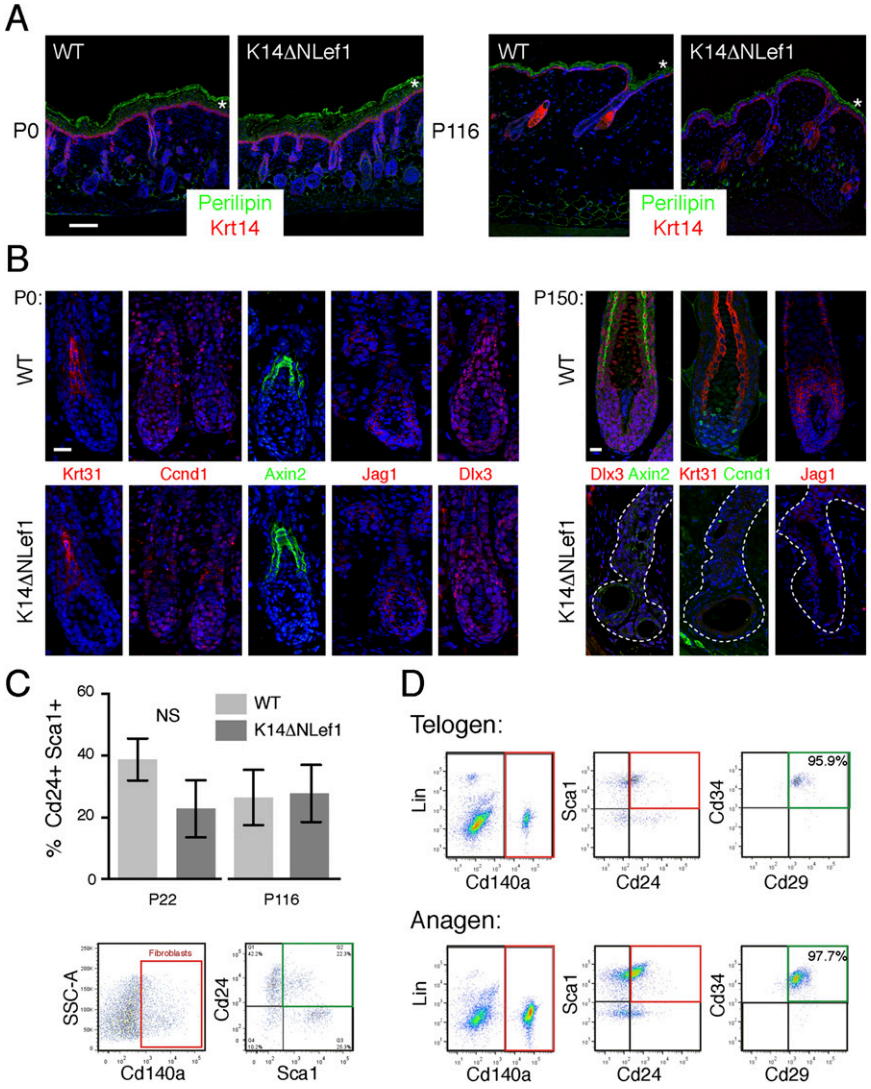


**Fig. S2.** K14ΔNLef-1 transgene does not affect adipogenesis during hair follicle morphogenesis. (*A*) Sections of WT and K14ΔNLef-1 postnatal day (P)0 and P116 skin were immunostained for Perilipin (green) and Krt14 (red), with DAPI counterstain (blue). (*B*) WT and K14ΔNLef-1 P0 (*Left*) and P150 (*Right*) skin sections immunostained with antibodies to Wnt/β-catenin target genes (1–5). (*C*) Flow cytometry of Sca1/Cd24 double-positive adipocyte precursor cells isolated at the end of HF morphogenesis (P22) and at P116 from WT and K14ΔNLef-1 skin. (*C, Lower,* and *D*) Dot plots showing flow cytometry profiles and gating. (*D*) Comparison of our flow strategy for adipocyte precursors and the strategy used by Festa et al. (6), originally described in Rodeheffer et al. (7). All of the Cd140a/Pdgfra-positive cells are Lin negative, whereas 96–98% of the Sca1/Cd24 double-positive cells are Cd29 and Cd34 positive. The data indicate that the cell population sorted by our strategy is negative for Lin and positive for Cd34, Cd29, Cd24, and Sca1. [Scale bars, 100 (*A*) and 20 μm (*B*).]


1. Pálmer HG, Anjos-Afonso F, Carmeliet G, Takeda H, Watt FM (2008) The vitamin D receptor is a Wnt effector that controls hair follicle differentiation and specifies tumor type in adult epidermis. *PLoS ONE* 3(1):e1483.
2. Estrach S, Ambler CA, Lo Celso C, Hozumi K, Watt FM (2006) Jagged 1 is a beta-catenin target gene required for ectopic hair follicle formation in adult epidermis. *Development* 133(22): 4427–4438.
3. Jho EH, et al. (2002) Wnt/beta-catenin/Tcf signaling induces the transcription of Axin2, a negative regulator of the signaling pathway. *Mol Cell Biol* 22(4):1172–1183.
4. Shtutman M, et al. (1999) The cyclin D1 gene is a target of the beta-catenin/LEF-1 pathway. *Proc Natl Acad Sci USA* 96(10):5522–5527.
5. Hwang J, Mehrani T, Millar SE, Morasso MI (2008) Dlx3 is a crucial regulator of hair follicle differentiation and cycling. *Development* 135(18):3149–3159.
6. Festa E, et al. (2011) Adipocyte lineage cells contribute to the skin stem cell niche to drive hair cycling. *Cell* 146(5):761–771.
7. Rodeheffer MS, Birsoy K, Friedman JM (2008) Identification of white adipocyte progenitor cells in vivo. *Cell* 135(2):240–249.

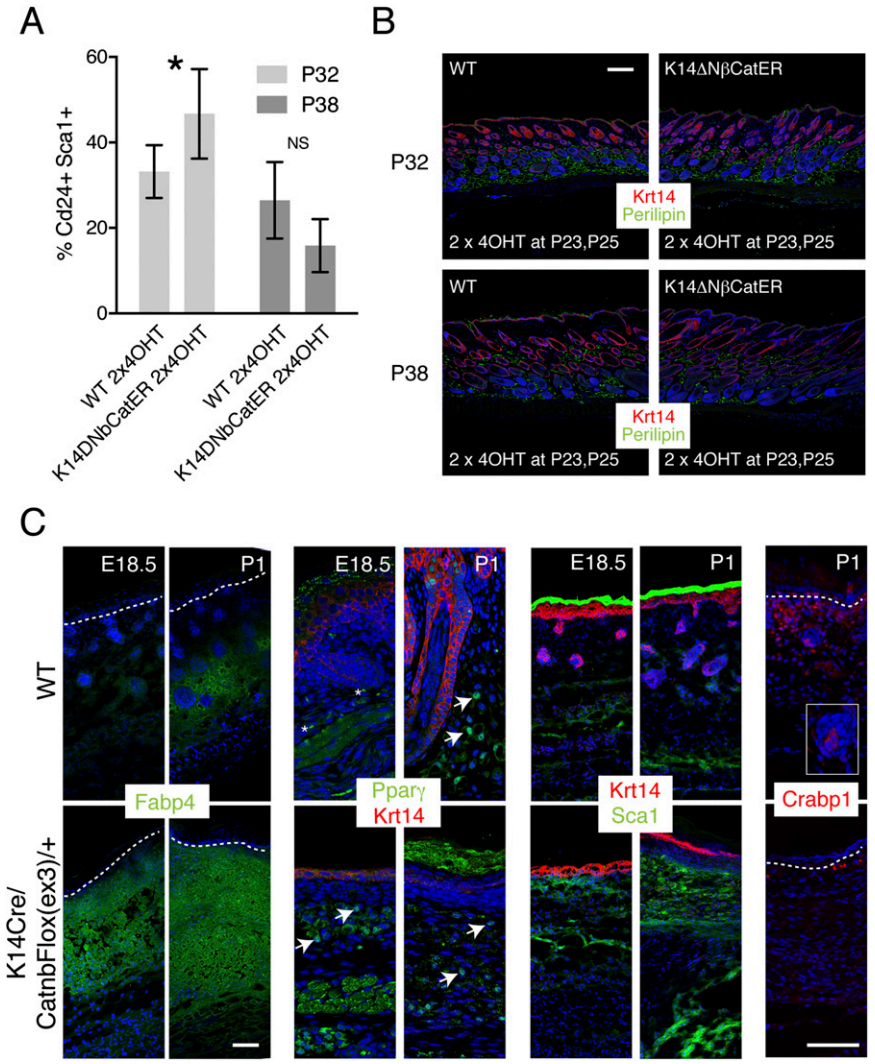


**Fig. S3.** Activation of Wnt/β-catenin signaling promotes dermal adipocyte formation during hair follicle morphogenesis. (*A*) Flow cytometry of Sca1/Cd24 double-positive adipocyte precursor cells at P32 and P38 in WT anagen and K14ΔNβ-cateninER anagen skin. Data are mean ± SD from five mice. $*P < 0.05$. (*B*) P32 and P38 WT anagen and K14ΔNβ-cateninER anagen skin sections were immunostained for Perilipin (green) and Krt14 (red), with DAPI counterstain (blue). (*C*) WT and K14Cre/CatnbFlox(ex3)/+ dorsal skin sections were immunostained for Fabp4, Pparγ, Sca1, and Crabp1. Dotted lines indicate position of basement membrane. White arrows indicate nuclear Pparγ. *White Inset* shows Crabp1 positive dermal papilla at higher magnification. (Scale bar, 100 μm.)

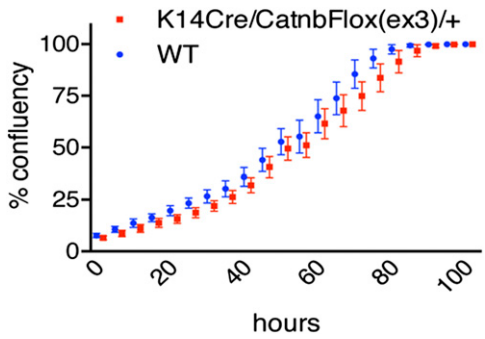


**Fig. S4.** Medium conditioned by K14Cre/catnbFlox(ex3)/+ and WT keratinocytes does not differentially affect 3T3-L1 preadipocyte growth rate. The percent confluence of 3T3-L1 cells cultured in the presence of conditioned medium from WT or K14Cre/CatnbFlox(ex3)/+ keratinocytes is shown. Data are mean ± SD from four independent wells.

**Table S1. Primer sequences (5′ to 3′)**

| Gene Name | Forward | Reverse |
|---|---|---|
| Leptin | GAGGAAAATGTGCTGGAGACC | GTGAAGCCCAGGAATGAAGTC |
| Adiponectin | TGGAGAGAAGGGAGAGAAAGG | GGTACATTGGGAACAGTGACG |
| Pparγ | ATAAAGTCCTTCCCGCTGACC | CTGGCACCCTTGAAAAATTCG |
| Fabp4 | GCTTGTCACCATCTCGTTTTC | TCACCATCCGGTCAGAGAGTA |
| Pref1 | GGAGAAAGGCCAGTACGAATG | CACAGAAGTTGCCTGAGAAGC |
| ActB | TGGCGTGAGGGAGAGCATAG | GCCAACCGTGAAAAGATGACC |